

# Recombinant Expression and Functional Characterization of Human Hephaestin: A Multicopper Oxidase with Ferroxidase Activity<sup>†</sup>

Tanya A. M. Griffiths, A. Grant Mauk, and Ross T. A. MacGillivray\*

Department of Biochemistry and Molecular Biology and Centre for Blood Research, University of British Columbia, Life Sciences Centre, 2350 Health Sciences Mall, Vancouver, British Columbia, Canada V6T 1Z3

Received August 4, 2005; Revised Manuscript Received September 8, 2005

**ABSTRACT:** Human hephaestin (Hp) is a transmembrane protein that has been implicated in duodenal iron export. Mutations in the murine *hephaestin* gene (*sla*) produce microcytic, hypochromic anemia that is refractory to oral iron therapy. Hp shares ~50% sequence identity with the plasma multicopper ferroxidase ceruloplasmin including conservation of residues involved in disulfide bond formation and metal coordination. On the basis of this similarity to ceruloplasmin, human hephaestin may also bind copper and possess ferroxidase activity. To test this hypothesis, human hephaestin cDNA has been cloned by reverse transcription of human duodenal mRNA. Following in vitro mutagenesis to make the encoded polypeptide suitable for expression and purification, the hephaestin cDNA was cloned into the expression vector pNUT and introduced into baby hamster kidney cells. After selection with methotrexate, the baby hamster kidney cells secreted the recombinant human hephaestin into the medium at a level of ~2 mg/L. Purification was achieved by a single immunoaffinity chromatography step. As judged by SDS–PAGE, N-terminal sequence analysis, and matrix-assisted laser desorption ionization-time-of-flight mass spectrometry, the purified hephaestin was homogeneous with a mass of 129600 Da, suggesting a carbohydrate content of 7.7%. Inductively coupled plasma mass spectrometry revealed that recombinant hephaestin contained an average of 3.13 atoms of copper per protein molecule. A visible absorption maximum was observed at 607 nm, consistent with the presence of a Type 1 copper site. By using ferrous ammonium sulfate as a substrate, recombinant hephaestin was shown to have ferroxidase activity with a  $K_m$  of 2.1  $\mu$ M for Fe(II). Lastly, urea PAGE showed that hephaestin was able to catalyze formation of diferric transferrin from Fe(II) and apotransferrin.

Several aspects of enteric iron absorption and transfer to blood remain poorly understood. Once inside the duodenal enterocyte, Fe(II) is transported from the apical to the basolateral side of the cell. As the cytoplasm favors the oxidation of Fe(II) to Fe(III), the Fe(II) is probably bound to a currently unidentified chaperone protein during this intracellular transport step. Once the Fe(II) reaches the basolateral plasma membrane, the Ireg1 transporter can function in the transport of Fe(II) into the blood plasma, but Fe(II) is not bound by apotransferrin, the transport protein of blood. Hence, ferroxidase activity on the basolateral membrane surface is believed to be essential in the transfer of iron from the mucosa to blood (for a review, see Aisen et al., 2001 (1)).

One potential candidate for this ferroxidase activity is ceruloplasmin (Cp).<sup>1</sup> Cp is the major copper binding protein in blood plasma and has been well characterized at the amino acid sequence (2), cDNA sequence (3), and gene (4) levels. The crystal structure of human Cp has demonstrated that this protein binds six integral copper atoms (5) that are distributed among three types of sites and that are necessary for the ferroxidase activity of the protein. Three copper atoms are found at three mononuclear Type 1 (T1) sites that give the protein a distinctive blue color ( $\lambda_{max} \sim 600$  nm,  $\epsilon \sim 7000$ – $9000$  M<sup>-1</sup> cm<sup>-1</sup>). One copper atom forms a Type 2 (T2) copper site, while two copper atoms form a Type 3 (T3) site in which the copper atoms are antiferromagnetically coupled and bridged by a hydroxyl group (6). The T2 and T3 sites form a functional unit referred to as the trinuclear cluster that is the site of dioxygen binding and reduction. Electron transfer from the Fe(II) substrate, likely bound near a T1 site (5, 7), to the T1 Cu(II) and ultimately to the trinuclear cluster results in the four-electron reduction of O<sub>2</sub> to 2H<sub>2</sub>O and oxidation of Fe(II) to Fe(III). Despite Cp possessing ferroxidase activity, there is no evidence to support a role for Cp as the intestinal ferroxidase (8).

An alternative candidate for this ferroxidase activity arose from two discoveries. First, a mouse mutant was described

<sup>†</sup> This work was supported in part by grants from the Canadian Blood Services – Canadian Institutes of Health Research Blood Utilization and Conservation Initiative (to R.T.A.M. and A.G.M.), a Canada Research Chair (to A.G.M.), and a Graduate Fellowship from the Strategic Training Program in Transfusion Science supported by the Canadian Institutes of Health Research and the Heart and Stroke Foundation of Canada (to T.A.M.G.). The spectrophotometer and mass spectrometer were funded by Canadian Foundation of Innovation grants to the UBC Centre for Blood Research and the UBC Laboratory of Molecular Biophysics.

\* To whom correspondence should be addressed. Tel. 604 822-3027. Fax: 604 822-4364. E-mail: macg@interchange.ubc.ca.

<sup>1</sup> Abbreviations: Cp, ceruloplasmin; Hp, hephaestin.

in 1962 that exhibited an X-linked, recessive hypochromic, microcytic anemia. The gene responsible for this disorder was called *sex-linked anemia* or *sla* (9). Subsequent studies showed that the anemia could be corrected by intraperitoneal delivery of Fe(II) but not by ingested iron (10) and that the *sla* mutation involved a defect in the transport of iron from the enterocyte to the blood plasma (11, 12). A potential consequence of this genetic defect could be the lack of ferroxidase activity that is required for production of Fe(III) as required for iron binding to apotransferrin.

The second discovery arose from genome sequencing projects in which a Cp homologue was identified on the mouse (13) and human (14) X chromosome. The predicted polypeptide encoded by the candidate gene shared 50% sequence identity with Cp, including the conservation of the cysteinyl residues involved in Cp disulfide bonding and the histidyl, cysteinyl, and methionyl residues involved in copper coordination. This candidate gene was called *hephaestin* (Hp) after the Greek god of metallurgy (13). Evidence supporting a role for Hp as the cause of the murine hypochromic, microcytic anemia came from the identification of a 582 nucleotide deletion in the Hp mRNA in the *sla* mouse (13). Subsequently, Frazer et al. (15) prepared an anti-peptide antibody to mouse Hp, and others have used this antibody to show that mouse enterocyte membranes contain a protein with ferroxidase activity that comigrates with Hp during PAGE (16). Syed et al. have used the sequence identity between Cp and Hp to construct a hypothetical structural model of Hp (14).

The current report describes the recombinant expression and functional characterization of human Hp. In particular, results of two types of assays are reported that establish that Hp does possess ferroxidase activity and that in the presence of Fe(II) and apotransferrin, Hp catalyzes the formation of diferric transferrin.

## MATERIALS AND METHODS

**Materials.** Coupling of the anti-1D4 monoclonal antibody (kindly provided by Dr. Robert Molday, Department of Biochemistry and Molecular Biology, University of British Columbia, Canada) to CNBr-activated Sepharose 4B (GE Healthcare, Piscataway, NJ) was carried out at a concentration of 2 mg/mL according to the supplier's instructions (GE Healthcare). Large unilamellar vesicles (LUVs) composed of equimolar amounts of DODAC/DOPE were kindly provided by Dr. Pieter Cullis (Department of Biochemistry and Molecular Biology, University of British Columbia). Expand High Fidelity *Taq* polymerase was obtained from Roche (Mississauga, ON). Ferrous ammonium sulfate hexahydrate (ReagentPlus grade) was obtained from Sigma-Aldrich (Oakville, ON). Peptide synthesis was performed by the Nucleic Acid Protein Service (NAPS) at the University of British Columbia, and oligonucleotide synthesis was performed by NAPS and Operon Biotechnologies (Huntsville, AL). DNA restriction and modification enzymes were from New England Biolabs (Beverly, MA). All polymerase chain reaction (PCR) and cloning steps were performed using established protocols (17). Amino-terminal sequence analysis and electrospray ionization/matrix-assisted laser desorption ionization-time-of-flight (MALDI-TOF) mass spectrometric analyses were carried out by the Laboratory of Molecular

Table 1: Oligonucleotides Used in This Study (shown 5' → 3')

Fragment 1F	CTGGACACGTAGAAAGCCCCTTTGTTC
Fragment 1R	ATTGCATGCATCCTATTGCTCTCCTGA
Fragment 2F	TGGGCCACTGAAAGCTGATGAC
Fragment 2R	CCCAGGATTCCAAGATGCCTATCT
Fragment 3F	GCTGAGATGGTGGCCTGGGAACC
Fragment 3R	TGTCAGGCTGCATGATGGCCA
Fragment 4F	CCATAAGAGACACAAATTCTGGCCTGGTG
Fragment 4R	CTCTGGGATGTTCCACTGATAAGTGACCAC
Fragment 5F	CATGCTCATGGAGTGCTAGAATCTACT
Fragment 5R	TACAGATGTGCTTCCTGAGGATATCTC

Biophysics Proteomics Core Facility, University of British Columbia. Amino acid analysis (AAA) was performed at the Protein Chemistry Laboratory, Texas A&M University.

**Isolation of Total RNA from Human Duodenum and First Strand Synthesis.** After obtaining informed consent for use in biomedical research, a sample of human duodenal tissue from a brain dead organ donor was kindly provided by Dr. Mark Meloche (Department of Surgery, University of British Columbia, Canada). Total RNA was isolated from the duodenal tissue using a TRIzol kit (Invitrogen, Burlington, ON) according to the supplier's recommendations. First strand cDNA synthesis was performed using 8 µg of total RNA, Superscript II Reverse Transcriptase (Invitrogen), and both pd(N)<sub>6</sub> random hexamers and (dT)<sub>12–18</sub> oligonucleotides (GE Healthcare) as primers according to supplier's suggestions.

**DNA Manipulation.** On the basis of homology of the Cp and Hp genes, the entire Hp cDNA was predicted to be 4854 bp in length (14). Five pairs of PCR primers were designed (Table 1) and used to amplify the Hp coding region in five overlapping fragments, each containing unique restriction sites (from 5' → 3': *Xma*I, *Sac*I, *Eco*RI, and *Bsp*I). Individual PCR products were purified using the QIAquick PCR Purification kit (Qiagen, Mississauga, ON), cloned in the pBluescriptII SK<sup>–</sup> (pBSSK<sup>–</sup>) vector (Stratagene, La Jolla, CA), and propagated in DH5α *Escherichia coli*. Plasmid DNA was purified using a QIAprep spin miniprep kit (Qiagen). Following subsequent restriction digests and ligations, the entire Hp coding region was assembled. To produce soluble Hp, five genetic engineering steps were completed: (i) the coding region for the native Hp signal peptide was removed and replaced with the signal peptide and the first four residues of human transferrin; (ii) the coding region for the putative C-terminal transmembrane region was removed by truncating Hp at amino acid Ser1070 (amino acid numbering according to NCBI Accession CAC35365); (iii) a FXa recognition sequence IEGR was introduced; (iv) the 1D4 epitope (18, 19) was introduced; and (v) *Not*I sites were incorporated into the 5' and 3' ends. The Hp-1D4 construct was excised from the pBSSK<sup>–</sup> vector via the 5' and 3' *Not*I restriction sites, ligated into the *Not*I digested pNUT vector (20), and propagated in DH5α *E. coli*. Automated DNA sequence analysis using the BigDye Terminator kit and an ABI 3700 DNA sequencer (Applied Biosystems, Streetsville, ON) was used to verify all constructs.

**Expression, Purification, and Characterization of Soluble Hp.** BHK cells were grown to confluence in six-well tissue culture plates in Dulbecco's modified Eagle's medium-Ham F12 nutrient mixture (DMEM-F12) containing 5% newborn calf serum (NCS) (Invitrogen) in a humidified 5% CO<sub>2</sub> atmosphere. Lipoplexes were formed by mixing 10 µg of plasmid DNA with 40 mM LUVs in 1% glucose in a total

volume of 500  $\mu\text{L}$ , and samples were incubated on ice for 20 min prior to use. Lipoplexes were added in a dropwise fashion directly to the cell medium that was bathing the cells. After incubation of the cells for 24 h, 0.44 mM methotrexate was added to the medium. Methotrexate-resistant colonies containing the pNUT plasmid were evident 10 days following selection, and these were expanded into flasks for transfer into roller bottles or frozen in a liquid nitrogen apparatus in 95% DMEM-F12-NCS-methotrexate medium/5% DMSO. Large scale cultures of BHK cells were grown in Corning expanded surface roller bottles (1700  $\text{cm}^2$ , Fisher Scientific, Ottawa, ON) at 37 °C in an ambient atmosphere. The culture medium (200 mL/bottle) was collected every 3 days. The first batch contained DMEM-F12, 5% NCS, and methotrexate, whereas subsequent batches contained DMEM-F12, 2% Ultrosor G (BioSeptra, Marlborough, MA), and 10  $\mu\text{M}$   $\text{CuSO}_4$ .

Hp was purified from 600 mL of culture medium within 24 h of collection. The medium was clarified by vacuum filtration through a 0.45  $\mu\text{m}$  cellulose filter (Millipore, Nepean, ON), brought up to pH 7.1, 10 mM Tris-HCl by the addition of 1 M Tris-HCl, pH 7.4 and passed through an anti-1D4 immunoaffinity CNBr-Activated Sepharose 4B column (bed volume, 10 mL;  $2 \times 3$  cm; 2.5 mL/min; 4 °C) that had been equilibrated with 10 mM Tris-HCl, pH 7.1, 150 mM NaCl. The column was washed with 20 bed volumes of the equilibration buffer. The bound protein was eluted at room temperature with  $5 \times 5$  mL volumes of the equilibration buffer containing 0.2 mg/mL of the 1D4 peptide (*N*-acetylation-TETSQVAPA). All eluants were combined and 10% SDS PAGE was used to establish that the Hp in this sample was >95% pure. Western blots directed against the 1D4 epitope tag were performed as previously described (21). Purified Hp was treated with Endo-H and PNGase F glycosidases as per the supplier's recommendation (New England Biolabs), and the deglycosylated Hp was visualized by 10% SDS PAGE. For long-term storage, purified Hp was concentrated to 10–30  $\mu\text{g}$  of protein/ $\mu\text{L}$  using Amicon Ultra-15 Centrifugal Filter Units (30 000 Da, NMWL) and Amicon Ultrafree-0.5 Centrifugal Filter Units (50 000 Da, NMWL) (Millipore) and snap-frozen in liquid nitrogen before storage at –70 °C.

**Analytical Methods.** Protein concentration was initially determined from quantitative amino acid hydrolysis. To ensure sample purity, immunoaffinity purified Hp was subjected to gel filtration chromatography on a Superose 12 column (GE Healthcare) prior to sample preparation for AAA. The experimental molar absorption coefficient for the absorbance at 280 nm was  $215\,474\text{ M}^{-1}\text{ cm}^{-1}$ , and this was used for subsequent protein concentration determinations. Purified Hp samples were separated by 10% SDS PAGE and transferred to a PVDF membrane in *N*-cyclohexyl-3-aminopropanesulfonic acid buffer for amino-terminal sequence analysis. MALDI-TOF MS analysis was performed with a Voyager DE-STR instrument. A sample of purified Hp (17  $\mu\text{M}$ ) was mixed 1:1 (v/v) with sinapinic acid and applied to the stainless steel MALDI target by the dried droplet technique. Analysis of copper content was performed by inductively coupled plasma MS (ICP MS) with a Perkin-Elmer, Sciex Elan 6000 instrument that was calibrated with the Instrument Calibration Standard 2 (SPEX Certiprep, Metuchen, NJ). Samples of Hp and copper-loaded human

transferrin (apotransferrin from Sigma-Aldrich was copper-loaded according to Garratt et al. (22)) were prepared for analysis by dilution in 1%  $\text{HNO}_3$  (Trace Metal Grade, Fisher Scientific), that was, in turn, prepared with glass-distilled water that had been polished with a Nanopure water purification system. A solution of this 1%  $\text{HNO}_3$  prepared with this polished water was used as a blank. All samples were spiked with a selenium internal standard (Sigma-Aldrich), and values were normalized to this internal standard. Although copper was of primary interest in the ICP MS experiments, the zinc content was also determined in both samples. The protein concentration of the samples was determined from  $A_{280}$  measurements using the molar absorption coefficient described above for recombinant Hp and  $93\,000\text{ M}^{-1}\text{ cm}^{-1}$  for human transferrin (23).

**Spectroscopy and Ferroxidase Activity.** UV/visible absorbance spectra were recorded with a Varian Cary 4000 spectrophotometer (25 °C). Oxidation of Fe(II) to Fe(III) by 0.2  $\mu\text{M}$  Hp was performed with the Fet3p ferroxidase assay described by de Silva et al. (24). The concentration of residual Fe(II) was determined from the absorbance of the ferrozine-Fe(II) complex ( $\epsilon_{562} = 27\,900\text{ M}^{-1}\text{ cm}^{-1}$ ) (25). Ferroxidase activity of Hp was also demonstrated by monitoring the incorporation of Fe(III) into human apotransferrin (Sigma-Aldrich). Reactions were carried out in 200  $\mu\text{L}$  of solution containing 6.25  $\mu\text{M}$  apotransferrin, 200  $\mu\text{M}$  ferrous ammonium sulfate, and 100  $\mu\text{M}$  sodium ascorbate in 100 mM sodium acetate trihydrate, pH 5.0. Reactions were initiated with the addition of 0.4  $\mu\text{M}$  Hp (except for two controls to which no Hp was added) and proceeded for 1–365 min at 37 °C. The reactions were stopped by transfer to –20 °C. Samples were analyzed by 6% urea PAGE to separate the apo-, mono-, and diferric transferrin species (26).

## RESULTS

**Expression and Purification of a Soluble Form of Recombinant Hp.** Human duodenal RNA was isolated, and following RT-PCR the Hp coding region was cloned into pBSSK<sup>+</sup>. During sequence verification of Hp cDNA, an ACA>GTA polymorphism was detected at positions 1328–1330 (nucleotide numbering according NCBI Accession AJ296162), changing the codon for Thr222 to Val. To express soluble Hp, the putative C-terminal transmembrane region was removed, truncating the Hp protein at Ser1070, which is one residue shorter than the human Cp protein as determined by a protein sequence alignment. A FXa cleavage site and a 1D4 recognition epitope were added in place of the C-terminal transmembrane region. Following expression of the Hp-1D4 construct, it was observed that recombinant Hp was not secreted into the tissue culture medium by the BHK cells but remained intracellular (data not shown). Because the natural Hp signal peptide may not direct the secretion of the recombinant Hp, the Hp signal peptide was replaced with the human transferrin signal peptide. Following expression of this construct in BHK cells, we obtained soluble, secreted Hp (Figure 1, lanes 1–4). Levels of recombinant Hp increased over time; this was noticeable when the serum replacement Ultrosor G was introduced (Figure 1, between lanes 2 and 3, denoted with arrow). As judged by Western blotting and SDS–PAGE, neither degradation nor heterogeneity of Hp was observed over time. Immunoaffinity purification was performed within 24 h of medium collection



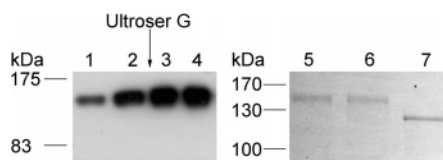


FIGURE 1: Western blot and glycosylation analyses of recombinant Hp. Medium from BHK cells expressing Hp was collected at days 4 (lane 1), 6 (lane 2), 9 (lane 3), and 12 (lane 4) post passage into roller bottles. Following 10% SDS-PAGE and transfer to a PVDF membrane, the blot was incubated with anti-ID4 primary antibody and anti-mouse secondary antibody and developed with ECL. One-step immunoaffinity purification resulted in Hp that was >95% pure (lane 5). Treatment with Endo-H (lane 6) did not affect the mass of Hp, while treatment with PNGase F (lane 7) caused a significant decrease in mass. Lanes 1–4 had equal volumes of sample loaded, but protein concentration was not determined. Lanes 5–7 had 2  $\mu\text{g}$  of total protein/lane.

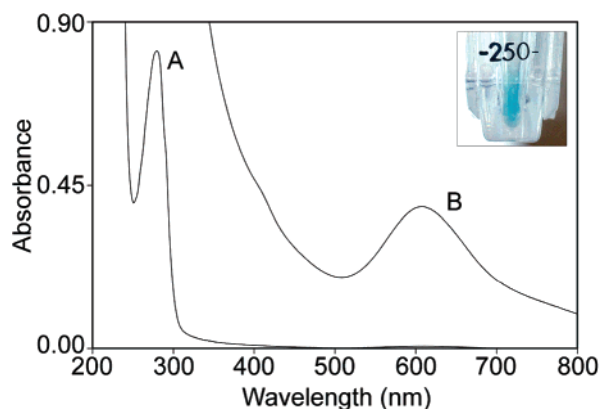


FIGURE 2: UV-visible spectrum of recombinant Hp. Trace A represents a 51-fold dilution of Hp (3.8  $\mu\text{M}$ ), while trace B is of undiluted Hp at a concentration of 194  $\mu\text{M}$ . Inset shows human Hp following purification and concentration (30  $\mu\text{g}$  of protein/ $\mu\text{L}$ ).

and required 1 day to complete; the binding and washing steps were performed at 4  $^{\circ}\text{C}$  to preserve both the antigen and antibody, while elution of Hp with the ID4 peptide was performed at room temperature. As judged by SDS PAGE, the Hp was >95% pure following this one-step purification (Figure 1, lane 5); no further purification was performed. Typically, the yield of pure Hp from 600 mL of medium was  $\sim 1$  mg.

**Characterization of Recombinant Human Hp.** The electronic spectrum of recombinant Hp exhibits a maximum at 607 nm (2010  $\text{M}^{-1}\text{cm}^{-1}$ , Figure 2) that is responsible for the anticipated blue color of Hp (Figure 2, inset). For multicopper oxidases with a single T1 site, the accepted absorption coefficient is 5000  $\text{M}^{-1}\text{cm}^{-1}$  (27). The amino-terminal sequence of recombinant Hp was determined by Edman degradation to be  $\text{NH}_2\text{-VPDKATRVY-}$ . This sequence is consistent with the cDNA sequence and represents the four amino-terminal residues of transferrin (VPDK) followed by the sequence of Hp starting at Ala24. Potential glycosylation of Hp was investigated by using specific endoglycosidases. Treatment of Hp (2  $\mu\text{g}$ ) with the endoglycosidase Endo-H and subsequent SDS PAGE did not result in a mobility shift, suggesting an absence of high mannose oligosaccharides (Figure 1, lane 6). PNGase F treatment of the same amount of Hp demonstrated a significant reduction in molecular mass from  $\sim 143$  kDa to  $\sim 121$  kDa (Figure 1, lane 7), suggesting cleavage of hybrid or complex N-linked oligosaccharides. Such heterogeneity of glycosylation is

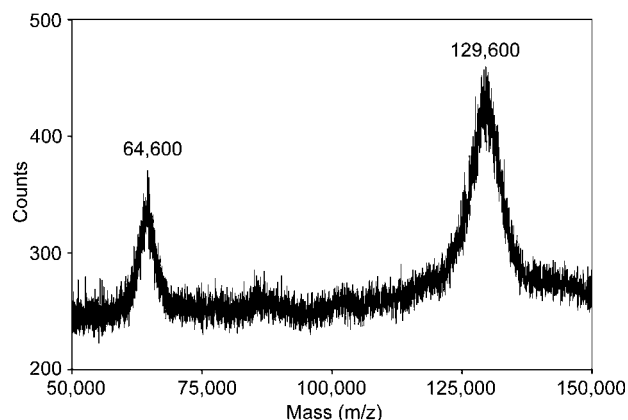


FIGURE 3: MALDI-TOF MS analysis of recombinant Hp. The Voyager DE-STR was calibrated externally with IgG. The peak at 64600 Da is the doubly charged species while the 129 600 Da species is singly charged recombinant Hp.

consistent with the complex and uninterpretable electrospray ionization MS analysis of recombinant Hp (data not shown). Therefore, MALDI-TOF MS analysis was used to determine the mass of recombinant Hp as 129 600 Da (Figure 3). ICP MS was used to determine the copper content of purified Hp using human transferrin loaded with copper as a control. Prior to analysis, all samples were spiked with a commercially available selenium standard, and values were normalized to this standard (results are the average of at least three analyses). Copper-loaded transferrin contained an average of  $1.98 \pm 0.04$  copper atoms per protein molecule; this result agrees well with the expected value of two Cu atoms/transferrin molecule (28). Hp was found to have an average of  $3.13 \pm 0.03$  copper atoms per protein molecule; based on the number of putative copper binding sites in the Hp sequence, the expected value is six Cu atoms/Hp molecule (14). A small amount of zinc ( $0.60 \pm 0.04$  Zn atoms per protein molecule) was also detected in the sample of recombinant Hp.

**Ferroxidase Activity.** Using Fe(II) as a substrate, the kinetic parameters of the ferroxidase activity of purified Hp were determined. Ferroxidase activity assay mixtures contained 0.2  $\mu\text{M}$  Hp ( $\sim 5$   $\mu\text{g}$ ) in 100 mM sodium acetate trihydrate/100  $\mu\text{M}$  sodium citrate buffer (pH 5.0, the optimal pH for Hp ferroxidase activity (data not shown), at room temperature). The reaction was initiated by the addition of varying concentrations of freshly prepared ferrous ammonium sulfate solution and was quenched by addition of ferrozine solution (15 mM) at 1 min intervals. Ferrozine is colorless, and the Fe(II)-ferrozine complex is a bright pink color; thus, substrate depletion was determined from the residual absorbance of the ferrozine-Fe(II) complex. Under these conditions, Fe(II) conversion to Fe(III) is irreversible, and Fe(III) does not inhibit the reaction so standard Michaelis–Menten analysis is appropriate (29). Heat inactivated recombinant Hp was used as a negative control, and as expected this protein exhibited no ferroxidase activity (data not shown). All ferroxidase reactions were corrected for background autooxidation rates of Fe(II). Thus, the kinetic parameters reported here represent the Hp catalyzed conversion of Fe(II) to Fe(III) (Figure 4A). An Eadie-Hofstee plot was used to determine the  $K_m$  (2.1  $\mu\text{M}$ ) and  $V_{\text{max}}$  (0.5  $\mu\text{M min}^{-1}$ ) for this reaction (Figure 4B). These parameters were then used to simulate the observed kinetic results (Figure

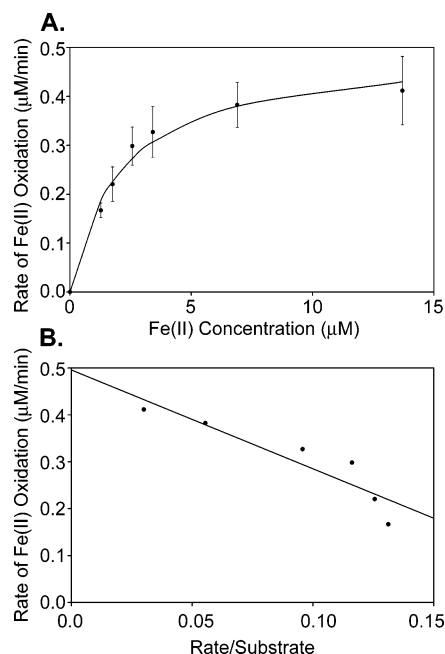


FIGURE 4: Ferroxidase activity of recombinant Hp. A discontinuous ferroxidase assay was performed to obtain the catalytic constants  $K_m$  and  $V_{max}$  for Hp. (A) Velocity versus substrate curve for Hp. Hp catalyzed oxidation of Fe(II) was determined as described. Reactions were quenched at 1 min intervals by the addition of ferrozine, and substrate depletion was measured at a wavelength of 562 nm using the molar absorptivity of the Fe(II)-ferrozine complex ( $\epsilon = 27\,900\text{ M}^{-1}\text{ cm}^{-1}$ ). Error bars represent 1 S.D. (B) Eadie-Hofstee plot used to determine  $K_m$  and  $V_{max}$  for the data shown in A.

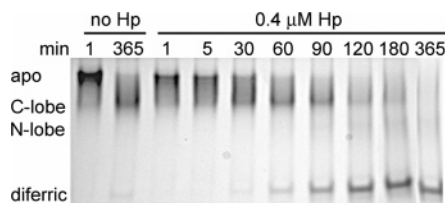


FIGURE 5: Oxidation of Fe(II) by Hp and incorporation of Fe(III) by human apotransferrin. Samples were incubated for the times indicated and analyzed by 6% urea PAGE to separate the apo-, mono-, and diferric transferrin species. Lanes 1 and 2 were controls to which no Hp was added. Lanes 3–10 were experimental samples that contained  $0.4\text{ }\mu\text{M}$  recombinant Hp.

4A, solid line). This model indicates that the data conform to Michaelis–Menten kinetics.

Roy and Enns (30) suggested that the intestinal ferroxidase activity of Hp may be necessary to facilitate the loading of apotransferrin with ferric iron for subsequent transport in blood to tissues. To assess this hypothesis, reaction mixtures containing apotransferrin and ferrous iron were incubated at  $37^\circ\text{C}$  for varying times in the presence or absence of Hp, and the reactions were then terminated by freezing at  $-20^\circ\text{C}$ . Samples were analyzed by urea PAGE, a technique that separates transferrin species based on ferric iron content (26). After more than 6 h at  $37^\circ\text{C}$  in the absence of Hp, very little apotransferrin was converted to mono- or diferric transferrin (Figure 5, lanes 1 and 2). As apotransferrin does not bind Fe(II), this result suggests that autooxidation of Fe(II) to Fe(III) during this reaction period was minimal. However, under the same experimental conditions but in the presence of Hp, more than half of the apotransferrin was

converted to mono- and diferric transferrin after 1 h, and conversion to diferric transferrin was complete after 365 min (Figure 5, lanes 3–10). These results establish that Hp catalyzes the oxidation of Fe(II) to Fe(III) and promotes the conversion of apotransferrin to diferric transferrin.

## DISCUSSION

The present study establishes that hephaestin, like ceruloplasmin (from blood plasma) and Fet3p (from yeast), is a multicopper oxidase with ferroxidase activity. Moreover, this activity has now been shown to promote efficient loading of apotransferrin with iron to form diferric transferrin. While ceruloplasmin is a soluble plasma protein, Hp and Fet3p are transmembrane proteins. Hp is present on the basolateral surface of duodenal enterocytes (31) and is thought to act in concert with the ferrous exporter, Ireg1 (1). Our goal was to express a secreted, soluble form of human Hp that could be purified in amounts sufficient for spectroscopic and kinetic analysis. This approach has previously proven to be successful for Fet3p (29). Truncation of the Hp construct to remove the putative transmembrane region was not sufficient for extracellular secretion, so the Hp signal peptide was replaced with that of human transferrin, a soluble plasma glycoprotein. This observation is consistent with that of Li and colleagues (32) who found that mouse Hp lacking the transmembrane domain was not secreted by *Saccharomyces cerevisiae*.

Following expression and secretion of Hp from the BHK cells, purification by elution over an anti-1D4 immunoaffinity column afforded convenient purification of the protein in a single day. Recombinant Hp exhibited no evidence of proteolytic degradation during purification, and the purified, concentrated protein retained activity after storage at  $-70^\circ\text{C}$  for at least 1 month. Notably, the arginyl and lysyl residues known to render human Cp (33) susceptible to proteolysis (34, 35) during purification (36) are not conserved in the sequence of Hp. Thus, Hp may prove to be a more robust multicopper oxidase for structural and kinetic studies.

**Mass Analysis.** The predicted mass of Hp with the first four amino acids of human transferrin and the FXa cleavage site/1D4 epitope is 119 580 Da. The mass of recombinant Hp obtained by MALDI-TOF analysis (Figure 2, 129 600 Da) is consistent with glycosylation of Hp. While recombinant Hp exhibited no change following treatment with the endoglycosidase Endo-H, treatment with PNGase F reduced the apparent mass of the protein (Figure 1, lanes 6 and 7). These observations suggest that recombinant Hp obtained as described in this work has been modified with hybrid or complex N-linked glycans. Related observations were reported by Nittis and Gitlin who found that endogenous human Hp from a colorectal adenocarcinoma cell line is synthesized as a single polypeptide and subsequently modified by PNGase F-sensitive N-linked glycans (37). Recombinant Hp has eight predicted N-linked glycosylation sites, but only two residues, N164 and N714, are probable candidates for glycosylation (<http://www.cbs.dtu.dk/services/NetNGlyc/> and ref 14). Recombinant Hp is unlikely to possess O-linked glycans (38), so the discrepancy between the experimental and predicted masses probably results from N-linked glycosylation or some additional form of posttranslational modification.

**Electronic Spectroscopy and Copper Content.** Purified Hp prepared in this work exhibited an absorbance maximum at 607 nm with a molar absorptivity of  $2010 \text{ M}^{-1} \text{ cm}^{-1}$  that is responsible for the blue color that is typical of multicopper oxidases and other proteins having a T1 copper site. As discussed above, Hp is predicted to have three T1 copper sites, so the low intensity of this maximum may be interpreted as indicating that only 10–15% of the T1 copper sites in the recombinant Hp are occupied. This conclusion is based on two assumptions: (1) the anticipated molar absorptivity of a single T1 copper site is  $\sim 4000\text{--}5000 \text{ M}^{-1} \text{ cm}^{-1}$  (27), and (2) all of the T1 copper sites in the Hp samples used to obtain the spectrum shown in Figure 2 were oxidized. Incomplete oxidation of the T1 copper sites of human Cp can result in a deceptively low molar absorptivity ( $7000 \text{ M}^{-1} \text{ cm}^{-1}$ ) that is increased to  $9000 \text{ M}^{-1} \text{ cm}^{-1}$  with the addition of oxidants (33). This resulting value for the human protein remains anomalously low apparently because one of the three T1 copper sites of human ceruloplasmin has a sufficiently high reduction potential that it is permanently reduced (39). Consequently, the molar absorptivity of the T1 maximum at 610 nm of human Cp is about one-third lower than that of chicken ceruloplasmin, a species of ceruloplasmin for which none of the three T1 copper sites has such a high reduction potential. Considering that the structural basis for the high potential T1 site of human Cp is the replacement of a Met ligand with a Leu residue (39) and that no sequence anomaly of this type pertains to human Hp, the presence of a permanently reduced T1 site in this protein seems highly unlikely.

ICP MS analysis of the recombinant Hp indicated the presence of an average of 3.13 copper atoms/protein molecule rather than the six copper atoms anticipated, yet Hp prepared in this manner possesses ferroxidase activity. As this activity presumably requires the presence of a trinuclear copper site and a minimum of one T1 copper, at least some of the Hp present in samples prepared as described here must possess a minimum of four copper ions distributed in this manner. It is possible that recombinant Hp has unoccupied copper binding sites or that other transition metals, such as zinc, nickel, or cadmium, have occupied the copper sites (40). Indeed, a small amount of zinc (a non-redox-active metal) was detected by ICP MS analysis in the recombinant Hp sample, although it is not clear where this zinc was bound to the protein. Our initial efforts to increase occupancy of copper binding sites in recombinant Hp by treatment with copper sulfate and ascorbate appeared to be unsuccessful (data not shown). In view of the apparent structural similarity of Hp and Cp and the complex procedure required for reconstitution of Cp with copper (41, 42), it is likely that reconstitution of Hp with copper will require a similarly complex protocol.

**Ferroxidase Activity.** Prior to this study, Hp was shown indirectly to possess oxidase activity toward both inorganic iron and organic amine-containing substrates (16). In this previous report, however, activity assays were not performed with purified Hp and kinetic parameters were not reported. We have used a discontinuous ferroxidase assay to determine the  $K_m$  and  $V_{max}$  of purified recombinant Hp with respect to ferrous ammonium sulfate as a substrate. The  $K_m$  observed here for Fe(II) is similar to previous observations for Fet3p ( $2.0\text{--}4.8 \mu\text{M}$ ) (24, 29), but the  $V_{max}$  for Hp is lower ( $0.5$

$\mu\text{M min}^{-1}$  versus  $1.0\text{--}1.8 \mu\text{M min}^{-1}$  for Fet3p). The low rate of Fe(II) oxidation observed here presumably results from insufficient copper incorporation into the recombinant Hp, consistent with the observation that addition of copper to recombinant Fet3p increased  $V_{max}$  without changing  $K_m$  (24).

The ferroxidase activity of Hp was also manifested by the ability of Hp to promote the formation of diferric transferrin on incubation of the protein with apotransferrin and Fe(II). Under identical conditions, incubation of apotransferrin and Fe(II) without Hp resulted in formation of little or no diferric transferrin (Figure 5). Given the localization of Hp to the basolateral membrane of duodenal enterocytes, this result is consistent with a role for Hp as the ferroxidase that catalyzes the oxidation of Fe(II) on the serosal side of the enteric epithelium for loading of Fe(III) onto apotransferrin. A possible requirement for physical interaction between the two proteins to facilitate iron transfer remains to be evaluated, but it is likely that Fe(III) released from Hp must be bound immediately by transferrin or another Fe(III) acceptor to avoid the consequences of the insolubility of Fe(III) at physiological pH and  $\text{O}_2$  concentrations (1). Further studies are required to determine the mechanism by which Fe(III) is transferred from Hp to apotransferrin.

## ACKNOWLEDGMENT

We thank Drs. Mark Meloche and Susan Curtis for their assistance in obtaining the human duodenal tissue, Dr. Richard Harrigan for access to automated DNA sequence analysis, Ms. Suzanne Perry for the MALDI-TOF MS analysis, and Ms. Chantal Levesque for her assistance with the ICP MS analysis.

## REFERENCES

1. Aisen, P., Enns, C., and Wessling-Resnick, M. (2001) Chemistry and biology of eukaryotic iron metabolism, *Int. J. Biochem. Cell Biol.* 33, 940–959.
2. Takahashi, N., Ortel, T. L., and Putnam, F. W. (1984) Single-chain structure of human ceruloplasmin: the complete amino acid sequence of the whole molecule, *Proc. Natl. Acad. Sci. U.S.A.* 81, 390–394.
3. Koschinsky, M. L., Funk, W. D., van Oost, B. A., and MacGillivray, R. T. (1986) Complete cDNA sequence of human preceruloplasmin, *Proc. Natl. Acad. Sci. U.S.A.* 83, 5086–5090.
4. Daimon, M., Yamatani, K., Igarashi, M., Fukase, N., Kawanami, T., Kato, T., Tominaga, M., and Sasaki, H. (1995) Fine structure of the human ceruloplasmin gene, *Biochem. Biophys. Res. Commun.* 208, 1028–1035.
5. Zaitseva, I., Zaitsev, V. N., Card, G., Moshkov, K., Bax, B., Ralph, A., and Lindley, P. F. (1996) The X-ray structure of human serum ceruloplasmin at 3.1 Å: nature of the copper centres, *J. Biol. Inorg. Chem.* 1, 15–23.
6. Solomon, E. I., and Lowery, M. D. (1993) Electronic structure contributions to function in bioinorganic chemistry, *Science* 259, 1575–1581.
7. Zaitsev, V. N., Zaitseva, I., Papiz, M., and Lindley, P. F. (1999) An X-ray crystallographic study of the binding sites of the azide inhibitor and organic substrates to ceruloplasmin, a multi-copper oxidase in the plasma, *J. Biol. Inorg. Chem.* 4, 579–587.
8. Hellman, N. E., and Gitlin, J. D. (2002) Ceruloplasmin metabolism and function, *Annu. Rev. Nutr.* 22, 439–458.
9. Falconer, D. S., and Isaacson, J. H. (1962) The genetics of sex-linked anemia in the mouse, *Genet. Res.* 3, 248–250.
10. Bannerman, R. M., and Cooper, R. G. (1966) Sex-linked anemia: a hypochromic anemia of mice, *Science* 151, 581–582.
11. Edwards, J. A., and Bannerman, R. M. (1970) Hereditary defect of intestinal iron transport in mice with sex-linked anemia, *J. Clin. Invest.* 49, 1869–1871.



12. Manis, J. (1971) Intestinal iron-transport defect in the mouse with sex-linked anemia, *Am. J. Physiol.* 220, 135–139.
13. Vulpe, C. D., Kuo, Y. M., Murphy, T. L., Cowley, L., Askwith, C., Libina, N., Gitschier, J., and Anderson, G. J. (1999) Hephaestin, a ceruloplasmin homologue implicated in intestinal iron transport, is defective in the sla mouse, *Nat. Genet.* 21, 195–199.
14. Syed, B. A., Beaumont, N. J., Patel, A., Naylor, C. E., Bayele, H. K., Joannou, C. L., Rowe, P. S., Evans, R. W., and Srai, S. K. (2002) Analysis of the human hephaestin gene and protein: comparative modelling of the N-terminus ecto-domain based upon ceruloplasmin, *Protein Eng.* 15, 205–214.
15. Frazer, D. M., Vulpe, C. D., McKie, A. T., Wilkins, S. J., Trinder, D., Cleghorn, G. J., and Anderson, G. J. (2001) Cloning and gastrointestinal expression of rat hephaestin: relationship to other iron transport proteins, *Am. J. Physiol. Gastrointest. Liver Physiol.* 281, G931–G939.
16. Chen, H., Attieh, Z. K., Su, T., Syed, B. A., Gao, H., Alaeddine, R. M., Fox, T. C., Usta, J., Naylor, C. E., Evans, R. W., McKie, A. T., Anderson, G. J., and Vulpe, C. D. (2004) Hephaestin is a ferroxidase that maintains partial activity in sex-linked anemia mice, *Blood* 103, 3933–3939.
17. Sambrook, J., and Russell, D. W. (2001) *Molecular Cloning: A Laboratory Manual*, 3rd ed., Cold Spring Harbor Laboratory Press, Cold Spring Harbor, NY.
18. Molday, R. S., and MacKenzie, D. (1983) Monoclonal antibodies to rhodopsin: characterization, cross-reactivity, and application as structural probes, *Biochemistry* 22, 653–660.
19. Hodges, R. S., Heaton, R. J., Parker, J. M., Molday, L., and Molday, R. S. (1988) Antigen–antibody interaction. Synthetic peptides define linear antigenic determinants recognized by monoclonal antibodies directed to the cytoplasmic carboxyl terminus of rhodopsin, *J. Biol. Chem.* 263, 11768–11775.
20. Palmiter, R. D., Behringer, R. R., Quaife, C. J., Maxwell, F., Maxwell, I. H., and Brinster, R. L. (1987) Cell lineage ablation in transgenic mice by cell-specific expression of a toxin gene, *Cell* 50, 435–443.
21. Wu, T. H., Ting, T. D., Okajima, T. I., Pepperberg, D. R., Ho, Y. K., Ripps, H., and Naash, M. I. (1998) Opsin localization and rhodopsin photochemistry in a transgenic mouse model of retinitis pigmentosa, *Neuroscience* 87, 709–717.
22. Garratt, R. C., Evans, R. W., Hasnain, S. S., Lindley, P. F., and Sarra, R. (1991) X.a.f.s. studies of chicken dicupric ovotransferrin, *Biochem. J.* 280, 151–155.
23. Li, H., Sadler, P. J., and Sun, H. (1996) Unexpectedly strong binding of a large metal ion ( $\text{Bi}^{3+}$ ) to human serum transferrin, *J. Biol. Chem.* 271, 9483–9489.
24. de Silva, D., Davis-Kaplan, S., Fergestad, J., and Kaplan, J. (1997) Purification and characterization of Fet3 protein, a yeast homologue of ceruloplasmin, *J. Biol. Chem.* 272, 14208–14213.
25. Brown, M. A., Stenberg, L. M., and Mauk, A. G. (2002) Identification of catalytically important amino acids in human ceruloplasmin by site-directed mutagenesis, *FEBS Lett.* 520, 8–12.
26. Mason, A. B., Miller, M. K., Funk, W. D., Banfield, D. K., Savage, K. J., Oliver, R. W., Green, B. N., MacGillivray, R. T., and Woodworth, R. C. (1993) Expression of glycosylated and non-glycosylated human transferrin in mammalian cells. Characterization of the recombinant proteins with comparison to three commercially available transferrins, *Biochemistry* 32, 5472–5479.
27. Solomon, E. I., Sundaram, U. M., and Machonkin, T. E. (1996) Multicopper Oxidases and Oxygenases, *Chem. Rev.* 96, 2563–2606.
28. Smith, C. A., Anderson, B. F., Baker, H. M., and Baker, E. N. (1992) Metal substitution in transferrins: the crystal structure of human copper-lactoferrin at 2.1-Å resolution, *Biochemistry* 31, 4527–4533.
29. Hassett, R. F., Yuan, D. S., and Kosman, D. J. (1998) Spectral and kinetic properties of the Fet3 protein from *Saccharomyces cerevisiae*, a multinuclear copper ferroxidase enzyme, *J. Biol. Chem.* 273, 23274–23282.
30. Roy, C. N., and Enns, C. A. (2000) Iron homeostasis: new tales from the crypt, *Blood* 96, 4020–4027.
31. Kuo, Y. M., Su, T., Chen, H., Attieh, Z., Syed, B. A., McKie, A. T., Anderson, G. J., Gitschier, J., and Vulpe, C. D. (2004) Mislocalisation of hephaestin, a multicopper ferroxidase involved in basolateral intestinal iron transport, in the sex linked anaemia mouse, *Gut* 53, 201–206.
32. Li, L., Vulpe, C. D., and Kaplan, J. (2003) Functional studies of hephaestin in yeast: evidence for multicopper oxidase activity in the endocytic pathway, *Biochem. J.* 375, 793–798.
33. Bielli, P., Bellenchi, G. C., and Calabrese, L. (2001) Site-directed mutagenesis of human ceruloplasmin: production of a proteolytically stable protein and structure–activity relationships of type 1 sites, *J. Biol. Chem.* 276, 2678–2685.
34. Kingston, I. B., Kingston, B. L., and Putnam, F. W. (1977) Chemical evidence that proteolytic cleavage causes the heterogeneity present in human ceruloplasmin preparations, *Proc. Natl. Acad. Sci. U.S.A.* 74, 5377–5381.
35. Dwulet, F. E., and Putnam, F. W. (1981) Complete amino acid sequence of a 50,000-dalton fragment of human ceruloplasmin, *Proc. Natl. Acad. Sci. U.S.A.* 78, 790–794.
36. Ryden, L. (1971) Evidence for proteolytic fragments in commercial samples of human ceruloplasmin, *FEBS Lett.* 18, 321–325.
37. Nittis, T., and Gitlin, J. D. (2004) Role of copper in the proteasome-mediated degradation of the multicopper oxidase hephaestin, *J. Biol. Chem.* 279, 25696–25702.
38. Julenius, K., Molgaard, A., Gupta, R., and Brunak, S. (2005) Prediction, conservation analysis, and structural characterization of mammalian mucin-type O-glycosylation sites, *Glycobiology* 15, 153–164.
39. Machonkin, T. E., Zhang, H. H., Hedman, B., Hodgson, K. O., and Solomon, E. I. (1998) Spectroscopic and magnetic studies of human ceruloplasmin: identification of a redox-inactive reduced Type 1 copper site, *Biochemistry* 37, 9570–9578.
40. Guzzi, R., Milardi, D., La Rosa, C., Grasso, D., Verbeet, M. P., Canters, G. W., and Sportelli, L. (2003) The effect of copper/zinc replacement on the folding free energy of wild type and Cys3Ala/Cys26Ala azurin, *Int. J. Biol. Macromol.* 31, 163–170.
41. Klemens, F. K., Severns, J. C., Tamilarasan, R., and McMillin, D. R. (1996) Aspects of the demetalation and remetalation of ceruloplasmin, *Inorg. Chim. Acta* 250, 75–79.
42. Musci, G., Di Marco, S., Bellenchi, G. C., and Calabrese, L. (1996) Reconstitution of ceruloplasmin by the Cu(I)-glutathione complex. Evidence for a role of  $\text{Mg}^{2+}$  and ATP, *J. Biol. Chem.* 271, 1972–1978.

BI051559K